Physical factors affecting the transport and fate of colloids in saturated porous media

Scott A. Bradford, Scott R. Yates, Mehdi Bettahar, and Jirka Simunek

George E. Brown, Jr., Salinity Laboratory, U.S. Department of Agriculture, Agricultural Research Service
Riverside, California, USA

Received 28 March 2002; revised 2 July 2002; accepted 2 July 2002; published 31 December 2002.

[1] Saturated soil column experiments were conducted to explore the influence of colloid size and soil grain size distribution characteristics on the transport and fate of colloid particles in saturated porous media. Stable monodispersed colloids and porous media that are negatively charged were employed in these studies. Effluent colloid concentration curves and the final spatial distribution of retained colloids by the porous media were found to be highly dependent on the colloid size and soil grain size distribution. Relative peak effluent concentrations decreased and surface mass removal by the soil increased when the colloid size increased and the soil median grain size decreased. These observations were attributed to increased straining of the colloids; i.e., blocked pores act as dead ends for the colloids. When the colloid size is small relative to the soil pore sizes, straining becomes a less significant mechanism of colloid removal and attachment becomes more important. Mathematical modeling of the colloid transport experiments using traditional colloid attachment theory was conducted to highlight differences in colloid attachment and straining behavior and to identify parameter ranges that are applicable for attachment models. Simulated colloid effluent curves using fitted first-order attachment and detachment parameters were able to describe much of the effluent concentration data. The model was, however, less adequate at describing systems which exhibited a gradual approach to the peak effluent concentration and the spatial distribution of colloids when significant mass was retained in the soil. Current colloid xfiltration theory did not adequately predict the fitted first-order attachment coefficients, presumably due to straining in these systems. *INDEX TERMS:* 1831 Hydrology: Groundwater quality; 1832 Hydrology: Groundwater transport

Citation: Bradford, S. A., S. R. Yates, M. Bettahar, and J. Simunek, Physical factors affecting the transport and fate of colloids in saturated porous media, *Water Resour. Res.*, *38*(12), 1327, doi:10.1029/2002WR001340, 2002.

1. Introduction

[2] Colloids are particles with effective diameters less than 10 μm [*McCarthy and Zachara*, 1989]. A variety of inorganic, organic, and microbiological colloids exist in natural subsurface systems including silicate clays, iron and aluminum oxides, mineral precipitates, humic materials, microemulsions of nonaqueous phase liquids, viruses, and bacteria. These colloid particles can be released into soil solution and groundwater through a variety of hydrologic, geochemical, and microbiological processes including translocation from the vadose zone [*Nyhan et al.*, 1985], dissolution of minerals and surface coatings [*Ryan and Gschwend*, 1990], precipitation from solution [*Gschwend and Reynolds*, 1987], deflocculation of aggregates [*McCarthy and Zachara*, 1989], and microbial mediated solubilization of humic substances from kerogen and lignitic materials [*Ouyang et al.*, 1996]. Consequently, colloid particles will vary widely in concentration, composition, structure, and size depending on the spatial and temporal variability of physical, chemical, and microbiological characteristics. The concentration of natural colloids in groundwaters typically ranges from 10^8 to 10^{17} particles L^{-1} [*Kim*, 1991].

[3] Knowledge of the processes that control colloid transport and fate is required to efficiently manage and remediate many environmental contaminants. For example, an accurate description of microbial (colloid) transport is required to assess contamination potential and to protect drinking water supplies from pathogenic microorganisms [*Bitton and Harvey*, 1992], in the development of engineered bioaugmentation and bioremediation strategies [*Wilson et al.*, 1986], and in microbially enhanced oil recovery [*MacLeod et al.*, 1988]. Furthermore, the high surface area of colloid particles facilitates the sorption of organic and inorganics contaminants such as polychlorinated biphenols (PCBs), polycyclic aromatic hydrocarbons (PAHs), heavy metals, and radionuclides [*Puls and Powell*, 1992]. The colloids can then act as a mobile solid phase that accelerates the transport of sorbed contaminants [*Ouyang et al.*, 1996].

[4] Colloids are affected by many of the same physical and chemical processes that influence solute transport, i.e., advection, diffusion, dispersion, and sorption. In the colloid transport literature, sorption processes are frequently alluded to as attachment, deposition, or filtration. In this manuscript, colloid sorption and desorption will be referred

to as attachment and detachment, respectively. Colloid attachment, the removal of particle mass from solution via collision with and fixation to the porous media, is typically assumed to be a primary process controlling colloid transport. Attachment is dependent on particle-particle, particle-solvent, and particle-porous media interactions including electrostatic, London–van der Waals, hydrodynamic, hydration (structural forces), hydrophobic, and steric interactions [*Elimelech and O'Melia*, 1990]. Colloid attachment is also reported to be influenced by the physically controlled processes of sedimentation and interception [*Logan et al.*, 1995]. The kinetics of particle attachment are controlled by the rate of transport to solid surfaces and subsequent fixation to these surfaces.

[5] Previous colloid transport studies in the literature have focused on the quantification of clean bed first-order attachment coefficients to describe particle removal in filter beds (porous media) [*Fitzpatrick and Spielman*, 1973; *Tobiason and O'Melia*, 1988; *Vaidyanathan and Tien*, 1991]. According to this approach, colloid removal by the filter bed decreases exponentially with depth. Colloid attachment theory also predicts an optimum particle size for transport for a given aqueous-porous medium system [*Tobiason and O'Melia*, 1988]. Smaller particles are predicted to be removed more efficiently by diffusive transport, and larger particles are predicted to be removed more efficiently by sedimentation and interception.

[6] Experimental observations of colloid transport are not always in agreement with colloid attachment theory. For example, researchers have reported enhanced colloid retention at the soil surface and that the spatial distribution of retained colloids does not follow a simple exponential decrease with depth [*Bolster et al.*, 1999; *Redman et al.*, 2001]. Some of these discrepancies have been attributed to soil surface roughness [*Kretzschmar et al.*, 1997; *Redman et al.*, 2001], charge heterogeneity [*Johnson and Elimelech*, 1995], and variability in colloid characteristics [*Bolster et al.*, 1999]. A time-dependent attachment rate has also been reported to occur as a result of differences in the attachment behavior of colloids on clean porous media and on media already containing attached colloids [*Johnson and Elimelech*, 1995]. Predicted attachment coefficients are also commonly underestimated when repulsive forces exist between the colloids and porous media [*Vaidyanathan and Tien*, 1991; *Ryan and Elimelech*, 1996].

[7] Some of the discrepancies between colloid transport data and attachment theory may also be due to the fact that colloid attachment theory does not account for straining. Straining is the trapping of colloid particles in the downgradient pore throats that are too small to allow particle passage [*McDowell-Boyer et al.*, 1986]. In contrast to colloid attachment, the process of colloid straining has received relatively little research attention. The magnitude of colloid retention by straining depends on both the colloid and porous medium properties. If the colloid particles are physically excluded from entering all of the soil pores, then complete straining (mechanical filtration) occurs [*McDowell-Boyer et al.*, 1986]. In this case, a filter cake or surface mat of colloids forms adjacent to the surface of the porous medium. This filter cake may significantly reduce the permeability of the porous medium-filter cake system [*Willis and Tosun*, 1980]. Incomplete straining occurs when colloids are physically excluded from pores that are smaller than some critical size. Hence colloid transport may occur in larger pores, and colloid retention may occur at pore throats and grain junctions that are below this critical size. Colloids retained in smaller pores decrease the effective pore size and may therefore increase subsequent particle retention in this pore. Incomplete straining has a finite capacity for particle accumulation and permeability reduction since colloids are retained in only part of the pore space.

[8] Natural porous media typically exhibit a wide range in pore sizes due to variations in grain size, orientation and configuration, and surface roughness. Few studies have, however, examined the influence of soil pore size distribution characteristics on colloid straining. It is possible that straining occurs at both the pore and grain scale. *Sakthivadivel* [1966, 1969] and *Herzig et al.* [1970] developed geometric relations between the effective diameter of colloids and soil grain size distribution characteristics to predict mass removal by straining and the resulting reduction in permeability. *Sakthivadivel* [1966, 1969] reported that straining was significant when the colloid diameter was greater than 5% of the median grain diameter of the porous medium. If an upper size limit equal to 0.01 mm (10 μm) is selected for colloids, then this finding indicates that straining will occur when the median grain size is less than 0.2 mm (sand soil texture). *Matthess and Pekdeger* [1985] generalized this rule to porous media made up of a distribution of grain sizes. Colloid transport data from *Harvey et al.* [1993], however, indicate that straining was more pronounced than predictions based upon the criteria given by *Matthess and Pekdeger* [1985]. *Harvey et al.* [1993] observed a trend of increasing colloid retention with increasing colloid size and hypothesized that migration of clay particles was responsible for this observed straining behavior.

[9] In principle, colloid straining is controlled only by the size of the colloid and the pore size distribution characteristics. Many chemical factors (i.e., pH, ionic strength, surface charge, etc.) will, however, affect the aggregating behavior of colloid particles (colloid size) and the effective pore size distribution. Colloids are stabilized when the electrical double layers are expanded and when the net particle charge does not equal zero [*Ouyang et al.*, 1996]. Increasing electrolyte concentration and ionic strength decreases the double layer thickness and thereby promotes colloid aggregation. Aqueous phase pH influences the net colloid and solid surface charge by changing pH dependent surface charge sites. *McCarthy and Zachara* [1989] also reported that monodispersed colloids may be produced through disaggregation if the ion balance is shifted from one dominated by divalent Ca^{2+} to one dominated by monovalent Na^{+}. These same chemical factors (pH, ionic strength, surface charge, and chemical composition) are also known to influence soil structure (disaggregation) and pore size distribution (shrinking and swelling) when the soil contains clays and other colloidal materials [*Ayers and Westcot*, 1989].

[10] The objective of this work is to investigate the influence of straining on colloid transport and fate in saturated porous media. For this purpose, soil column experiments were conducted for a variety of soil grain size distribution characteristics and colloid sizes. Colloid trans-

port and fate was assessed by measuring temporal changes in colloid effluent concentrations and the final spatial distribution of colloid particles remaining in the soil columns. These data were interpreted with the aid of conservative tracer (bromide) studies conducted simultaneously on the same soil columns and numerical modeling of the experimental systems.

2. Theory

[11] Colloid transport and fate models commonly employ a modified form of the advective-dispersive equation which incorporates colloid attachment theory [*Harvey and Garabedian*, 1991; *Corapcioglu and Choi*, 1996; *Bolster et al.*, 1999; *Schijven and Hassanizadeh*, 2000]. In the absence of colloid inactivation or degradation, the colloid mass transfer term between the aqueous and solid phases (E_{sw}) [N T^{-1} L^{-3}; N, T, and L denote number of colloid particles, time, and length, respectively] is frequently given as

$$E_{sw} = -\frac{\partial(\rho_b S)}{\partial t} = -\theta_w k_{\mathrm{att}} C + \rho_b k_{\mathrm{det}} S. \quad (1)$$

Here ρ_b [M L^{-3}; M denotes mass] is the soil bulk density, S [N M^{-1}] is the solid phase colloid concentration, t [T] is time, C [N L^{-3}] is the aqueous phase colloid concentration, θ_w [-] is the volumetric water content, k_{att} [T^{-1}] is the first-order colloid attachment coefficient, and k_{det} [T^{-1}] is the first-order colloid detachment coefficient. Colloid filtration theory is incorporated into the k_{att} term as [e.g., *Logan et al.*, 1995]

$$k_{\mathrm{att}} = \frac{3(1-\theta_w)}{2d_{50}} \eta \alpha v, \quad (2)$$

where η [ ] is the collector (porous medium) efficiency, α [ ] is the colloid sticking efficiency, d_{50} [L] is the median porous medium grain diameter, and v [L T^{-1}] is the pore water velocity. The collector efficiency accounts for colloid removal due to diffusion, interception, and gravitational sedimentation [*Logan et al.*, 1995]. The value of η is frequently calculated using the following correlation written in terms of dimensionless variables [*Logan et al.*, 1995; *Rajagopalan and Tien*, 1976]:

$$\eta = 4A_s^{1/3} N_{Pe}^{-2/3} + A_s N_{Lo}^{1/8} N_R^{15/8} + 0.00338 A_s N_G^{1.2} N_R^{-0.4}. \quad (3)$$

Here A_s is the Happel correction factor, N_{Pe} is the Peclet number, N_{Lo} is London-van der Waals attractive forces number, N_R is the interception number, and N_G is the gravitional number. The value of α represents the fraction of particles colliding with the porous media that remain attached and therefore reflects the net effect of repulsive and attractive forces between colloids and solid surfaces. The value of α is usually derived from experimental breakthrough curves [*Pieper et al.*, 1997; *Ryan et al.*, 1999] or from fitted values of k_{att} and calculated values of η [*Bales et al.*, 1991; *Redman et al.*, 1997].

3. Materials and Methods

[12] Fluorescent latex colloids (Interfacial Dynamics Company, Portland, Oregon) were used as model colloid particles in the experimental studies presented herein. These spherical colloid particles have been employed in previous colloid transport studies reported in the literature [*Elimelech and O'Melia*, 1990; *Wan and Wilson*, 1994a, 1994b; *Reimus*, 1995]. Yellow-green colloids (excitation at 490 nm and emission at 515 nm) were chosen because they can be more efficiently illuminated than other color types. Colloid sizes (0.45, 1.0, 2.0, and 3.2 μm) were selected to be consistent with sizes of typical pathogenic bacteria. These colloids have carboxyl surface functional groups grafted onto latex particle surfaces by the manufacturer to create a negatively charged hydrophobic colloid surface.

Table 1. Carboxyl Colloid Properties

d_p, μm	ρ_p, g cm^{-3}	ρ_q, μC cm^{-2}	C_i, particles l^{-1}	ϕ_w, deg	ζ, mV
0.45	1.055	14.6	4.24×10^{11}	115.2	N/M[a]
1.00	1.055	27.0	3.86×10^{10}	115.2	−77.33
2.00	1.055	27.8	4.85×10^{9}	115.2	−71.37
3.20	1.055	11.9	1.18×10^{9}	115.2	−57.25

[a]Not measured.

[13] Specific physical and chemical characteristics for the colloids are given in Table 1. Here d_p denotes the median diameter of the colloid particle, ρ_p is the particle density, ρ_q is the particle surface charge density, θ_w is the air-water contact angle, and ζ is the zeta potential. The values of d_p, ρ_p, and ρ_q were provided by the manufacturer. The reported uniformity of the colloid size distribution was verified for the 3.2 μm particles using a Coulter Counter (Beckman Coulter Inc., Fullerton, California). Good agreement was observed between the measured and the reported colloid size distribution. The value of θ_w was measured (average of five measurements) on a bed of 0.11 μm carboxyl latex colloids using a Tantec Contact Angle Meter (Tantec Inc., Schaumburg, Illinois). This bed was created following a protocol similar to that presented by *Wan and Wilson* [1994b]; i.e., several drops of concentrated colloid solution were placed on a microscope slide, fluid was distributed on the slide by tilting, and excess water was allowed to evaporated from the surface. The zeta potential was measured using a Zeta-meter 3.0 (Zeta-meter, Inc., Staunton, Virginia); i.e., measured electrophoretic mobility was converted to zeta potential using the Smoluchowski equation. The initial influent colloid concentration (C_i) used in the soil column experiments is also given in Table 1. These concentrations were selected to minimize any permeability reductions in the soils [*Sakthivadivel*, 1966, 1969; *Herzig et al.*, 1970] and to provide each column with a nearly equal mass of colloids (approximately 3.28 mg).

[14] The aqueous phase chemistry (pH, ionic strength, and composition) of the tracer, resident, and eluant solutions utilized in the soil column experiments was chosen to create a stabilized monodispersed suspension with the selected colloids. The initial resident and eluant solutions consisted of a 0.001 M NaCl with its pH buffered to 6.98 using $NaHCO_3$ (5×10^{-5} M). The colloid-conservative tracer solution consisted of 0.001 M NaBr with its pH buffered to 6.73 using $NaHCO_3$ (5×10^{-5} M) and the indicated initial colloid concentration listed in Table 1. The aqueous solvent in all the experimental solutions consisted of deaired (boiled) deionized water.

[15] Glass beads (USF Surface Preparation, Rancho Dominguez, California) and various sieve sizes of Ottawa

Table 2. Porous Medium Properties

	F20–F30	F35	F50	F70	F110	d_{50}, mm	U_i
2030	100%	-	-	-	-	0.71	1.21
3550	-	50%	50%	-	-	0.36	1.88
70110	-	-	-	50%	50%	0.15	2.25
MIX	-	25%	25%	25%	25%	0.24	3.06
GB	-	-	-	100%	-	0.26	1.20

sand (U.S. Silica, Ottawa, Illinois) were used in the soil column experiments. The Ottawa sands were selected as a representative aquifer material and to encompass a range in soil grain size distribution characteristics. The various Ottawa sands will be designated herein as 2030, 3550, MIX, and 70110, whereas glass beads will be denoted as GB. Table 2 summarizes the grain size distribution properties for the various porous media used in the soil column experiments. The median grain size (d_{50}; mm) and the uniformity index ($U_i = d_{60}/d_{10}$) are measures of the average grain size and the distribution of grain sizes, respectively; here x% of the mass is finer than d_x.

[16] *Bradford and Abriola* [2001] presented capillary pressure-saturation curves for the 2030, 3550, MIX, and 70110 Ottawa sands. An estimate of the pore size distribution of drained pores can be obtained from capillary pressure-saturations curves using Laplace's equation of capillarity. According to this approach, the drained pores for the various Ottawa sands were all larger than 10 μm in diameter. Smaller pores that may produce colloid straining could not be characterized by this method. The measured residual saturations do, however, provide an estimate of the volume fraction of the pore space that has pores less than 10 μm in diameter. The reported residual saturation values suggest that 2, 6.5, 16, and 30% of the pore space contain pores less than 10 μm in diameter for the 2030, 3550, MIX, and 70110 sands, respectively. In contrast, the criteria presented by *Matthess and Pekdeger* [1985] indicate that straining will not occur for the porous media and colloid sizes considered in this work.

[17] Ottawa sands typically consist of 99.8% SiO_2 (quartz) and trace amounts of metal oxides, are spheroidal in shape, and may have rough surfaces. In contrast, glass beads are relatively chemical homogeneous, spherical, and smooth. Hence glass beads serve as a control medium to minimize variations in chemical composition and surface roughness. The glass beads, Ottawa sands, and the carboxyl colloids (Table 1) possess a net negative surface charge at a neutral pH. Hence attractive electrostatic interactions between the colloids and the vast majority of the porous media are minimal. Attractive electrostatic interactions, however, can occur between the carboxyl colloids and the minor fraction of positively charged metal oxide surfaces distributed on the Ottawa sands.

[18] Aluminum soil columns, 10 cm long and 5 cm inside diameter, were used in the colloid transport studies that employed glass beads as the porous medium. These columns were equipped with standard fittings and stainless steal wire screen at both of their ends. The soil columns employed with Ottawa sands were 15 cm long and 4.8 cm inside diameter Kontes Chromaflex chromatography columns (Kimble/Kontes, Vineland, New Jersey) made of borosilicate glass. The chromatography columns were equipped with a standard flangeless end fitting at the column bottom and a flow adapter at the top. The flow adapter allowed the column bed length to be adjusted, thereby facilitating the tight sealing of the adapter at the soil surface. The manufacturer's bed support at the column inlet and outlet was replaced with a stainless steal wire screen (105 μm mesh spacing) supported by a coarser polyethylene screen to uniformly distribute water flow and colloids at the soil surfaces. Tubing to and from the columns, fittings, column O-rings, and flow adapter were composed of chemically resistant materials such as Teflon, viton, stainless steal, and Kalrez.

[19] The glass beads were thoroughly cleaned and dried before packing them in the soil columns. The cleaning procedure consisted of washing with distilled water, followed by ultrasonic cleaning in heated water for 30 min. In contrast, the Ottawa sands were used as provided by the

Table 3. Soil Column Properties (Darcy Velocity, q; Porosity, ε; and Column Length, L), Colloid Release Efficiency (E_r), and the Recovered Effluent (M_E), Soil (M_S), and the Total Colloid Mass Fraction (MB_T)

Soil Type	d_p, μm	q, cm min^{-1}	ε	L, cm	E_r	M_E	M_S	MB_T
2030	0.45	0.100	0.367	13.178	0.660	0.896	0.109	1.005
2030	1.00	0.101	0.378	13.420	0.780	0.825	0.075	0.900
2030	2.00	0.103	0.369	12.224	0.650	0.468	0.368	0.836
2030	3.20	0.103	0.362	13.069	0.590	0.440	0.637	1.077
3550	0.45	0.099	0.341	12.657	0.680	0.838	0.151	0.989
3550	1.00	0.100	0.342	12.672	0.840	0.872	0.103	0.975
3550	2.00	0.102	0.343	12.811	0.670	0.261	0.522	0.783
3550	3.20	0.102	0.341	12.774	0.630	0.342	0.728	1.070
MIX	0.45	0.104	0.328	12.407	0.660	0.958	0.215	1.173
MIX	1.00	0.105	0.330	12.459	0.810	0.843	0.181	1.024
MIX	2.00	0.107	0.344	12.672	0.600	0.115	0.969	1.084
MIX	3.20	0.108	0.336	12.533	0.610	0.118	1.254	1.372
70110	0.45	0.110	0.342	12.676	0.610	0.660	0.321	0.981
70110	1.00	0.106	0.342	12.676	0.800	0.463	0.430	0.893
70110	2.00	0.109	0.351	12.978	0.590	0.072	0.956	1.028
70110	3.20	0.110	0.356	12.948	0.610	0.028	0.884	0.912
GB	0.45	0.138	0.377	10.000	0.800	0.628	0.386	1.014
GB	1.00	0.152	0.360	10.000	0.751	0.232	0.794	1.026
GB	2.00	0.169	0.373	10.000	1.000	0.161	0.579	0.740
GB	3.20	0.145	0.369	10.000	0.863	0.006	1.268	1.274

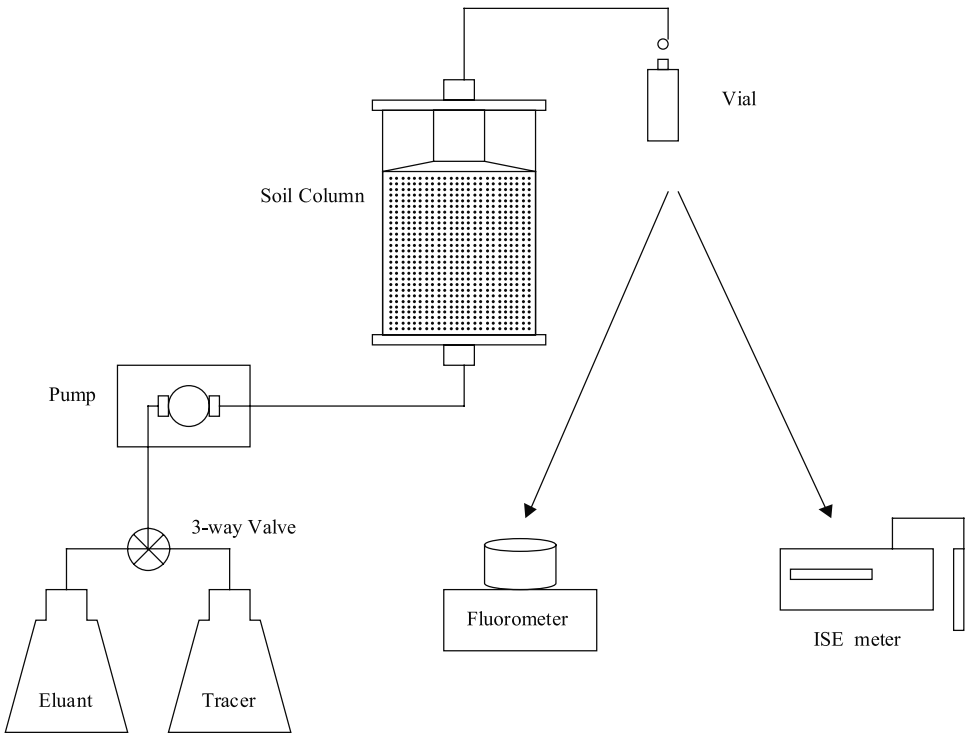

Figure 1. Schematic of the experimental setup employed in the colloid transport studies.

supplier. The soil columns were wet packed with the various porous media; i.e., the water level was always kept a few centimeters above the soil surface. Care was taken to ensure a uniform packing by completely mixing small quantities of the appropriate sieve size before addition to the columns. After each incremental addition of soil, the added soil was gently mixed with the lower surface layer of soil and then vibrated to minimize any settling and layering, and to liberate any entrapped air. Table 3 provides porosity (ε) values for each experimental soil column. The porosity was determined according to the method of *Danielson and Sutherland* [1986] using the measured soil bulk density and assuming a specific solid density of 2.65 g cm^{-3}.

[20] Before initiating a carboxyl colloid tracer experiment the soil columns containing Ottawa sand were flushed with several pore volumes (PV) of eluant solution to remove natural colloids particles from the porous media. A more rigorous procedure was used for the 2.0 and 3.2 μm carboxyl colloid experiments in 3550, MIX, and 70110 sands. For these soils and colloid sizes the analytic procedure was more sensitive to natural background colloids levels; i.e., low fluorescence readings were influenced by the sample optical density. In this case, the soil columns were flushed as follows: Initial resident solution was 0.026 M NaCl, 2 PV flush with deionized water, 2 PV flush with 0.026 M NaCl solution, 2 PV flush with deionized water, and finally a 4 PV flush with eluant solution. Here the 0.026 M NaCl solution promotes clay aggregation and the deionized water promotes clay mobilization [*Bettahar et al.*, 1998].

[21] Figure 1 is a schematic of the experimental setup employed for the colloid transport studies. A Masterflex L/S multihead drive pump (Barnant Company, Barrington, Illinois) equipped with standard heads was used to pump colloid and bromide tracer (colloids + 0.001 M NaBr + 5×10^{-5} M $NaHCO_3$) or eluant (0.001 M NaCl + 5×10^{-5} M $NaHCO_3$) solution upward through the vertically oriented columns at a steady rate. The average aqueous Darcy velocity (q) for the various soil column experiments is given in Table 3. The solution was pumped upward to minimize any sedimentation that may occur as a result of the difference in density of the colloid particles (density equals 1.055 g cm^{-3}) and water (density equal to 0.998 g cm^{-3}). The colloid and bromide tracer solution was pumped through the columns for around 77 min, after which a three-way valve was used to switch the pumped solution to the eluant (0.001 M NaCl + 5×10^{-5} M $NaHCO_3$) for a total experiment time of 250 min. A total of 50 effluent samples were collected in 20 mL glass scintillation vials over the course of each soil column experiment. Each sample was gathered during a 5-min time interval and then capped. The effluent colloid (particles L^{-1}) concentration was then determined on these samples using a Turner Quantech Fluorometer (Barnstead/Thermolyne, Dubuque, Iowa) equipped with excitation (490 nm, LE1095 $\times$ 13, NB490) and emission (515 nm, LE1095 $\times$ 23, SC515) filters. Some of these samples were also analyzed for bromide (mol L^{-1}) using an Orion 720a pH/ISE meter (Orion research Inc., Beverly, Massachusetts) equipped with an ion specific electrode for bromide. Colloid (average of triplicate measurements) and bromide concentrations were determined using linear calibration curves established between instrument response and standard solutions. The established calibration curves always had correlation coefficients very close to unity. This analytic protocol was sensitive to concentrations over 2 orders of magnitude below the initial colloid and bromide concentrations.

[22] Following completion of the colloid transport experiments, the spatial distribution of colloids in a soil column was determined. The end fitting was removed and the saturated

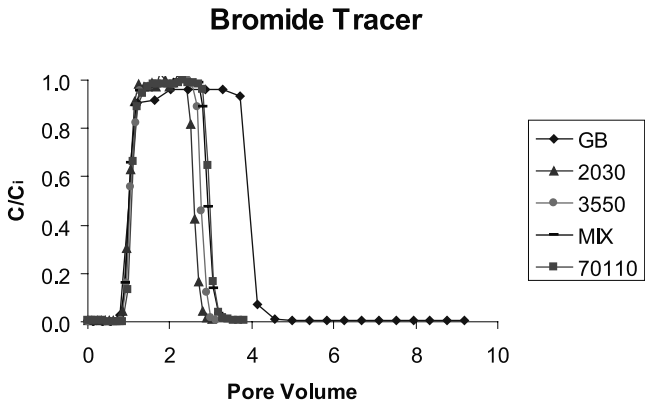

Figure 2. Representative plots of relative bromide concentration in the effluent versus pore volume for the indicated soil types.

porous media was carefully excavated into 20 mL scintillation vials or 50 mL glass centrifuge tubes. Around 16 vials (or eight centrifuge tubes) were used to recover the soil mass from a particular column. Excess eluant solution was added to fill the vials or centrifuge tubes. These vials or tubes were slowly shaken for 4 hours using a Eberbach shaker (Eberbach corporation, Ann Arbor, Michigan) to liberate strained colloids; this equilibration time interval was selected to be consistent with the duration of the colloid transport experiments. The concentration of the colloids in the excess aqueous solution (decanted from the vials) was measured using the Turner Quantech Fluorometer and the same experimental protocol outlined for the effluent samples. Water and sand filled vials (uncapped) were covered with aluminum foil (to prevent loss of sand from the vials) and placed in an oven for several hours to volatilize all of the remaining water from the sand. The volume of water and mass of sand in each vial or tube was determined from mass balance by measuring the weight of the empty vials (or tubes), water and sand filled vials, and sand filled vials.

[23] Duplicate "blank" soil column experiments were run for the various Ottawa sands to elucidate the influence of background clay colloids on the measured spatial distribution of 2.0 and 3.2 μm carboxyl colloids in 3550, MIX, and 70110 sands. These blank soil columns were subjected to the same cleaning, tracer, and excavation procedures and protocols given above. The only difference was that carboxyl colloids were not added to the columns. Background clay concentrations were determined from these blank soil columns at the column inlet, outlet, and middle. The average background concentration (a few percent, 2–8% in the aqueous phase) for a particular soil type was then subtracted off the corresponding measured 2.0 and 3.2 μm carboxyl concentrations determine from excavated soil.

[24] The release efficiency (E_r) of the carboxyl colloids from the porous media was sometimes less than 100% due to colloid attachment and/or straining. Colloid release efficiency was measured by placing a 10 g sample of dry porous media and 10 mL of colloid tracer solution at a specified concentration (100, 75, 50, 25, and 0% percent of C_i) into a 20 mL scintillation vial. These vials were shaken for 4 hours using an Eberbach shaker, and the concentration of the colloids in the aqueous solution was then measured using the Turner Quantech Fluorometer. Release efficiencies were determined as the ratio of the final and initial aqueous colloid concentrations. Table 3 presents the measured average release efficiencies for the various colloids and porous media. The measured colloid concentrations from excavated soil were corrected by dividing by the release efficiency.

[25] At the end of a soil column experiment, a colloid mass balance was conducted using effluent concentration data and the final spatial distribution of strained colloids in the sands. The calculated number of effluent and soil colloid particles was normalized by the total number of injected particles into a column for this purpose. Table 3 presents the recovered colloid mass fraction in the effluent (M_E) and soil (M_S), as well as the total (effluent + soil) colloid mass balance (MB_T). The value of M_S reflects uncertainty in the release efficiency and the background concentration of natural clay particles. Hence errors in MB_T are believed to be primarily caused by errors in M_S. In general, the values of MB_T are reasonably close to unity.

4. Results and Discussion

4.1. Bromide Effluent Concentration Curves

[26] Figure 2 presents representative plots of the relative bromide concentration (C/C_i) in the effluent versus pore volume (product of column volume and porosity) of water passing through the soil column for the indicated porous media. Observe that bromide serves as a good conservative tracer; i.e., bromide samples all of the pore water velocity distribution and moves at the average pore water velocity. Note also that the bromide breakthrough curves are very symmetric, indicating that physical nonequilibrium is not significant for bromide in these soil column experiments.

4.2. Colloid Effluent Concentration Curves

[27] Figure 3 presents a plot of the relative colloid concentration in the effluent as a function of pore volume for the indicated colloid sizes in the glass beads. Also shown in this figure is a plot of a representative bromide effluent concentration curve in the glass beads. Observe that the break-

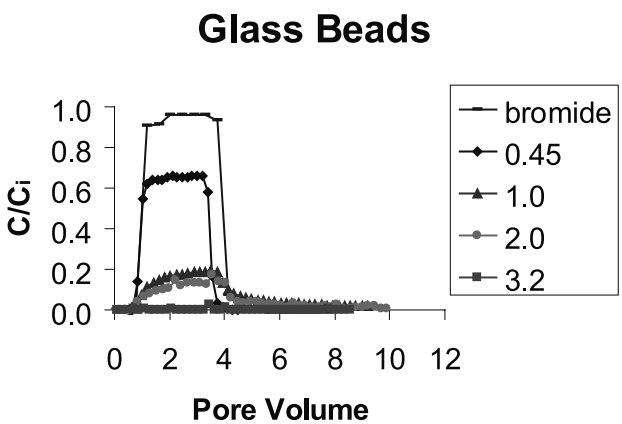

Figure 3. A plot of the relative colloid concentration in the effluent as a function of pore volume for the indicated colloid sizes in the glass beads.

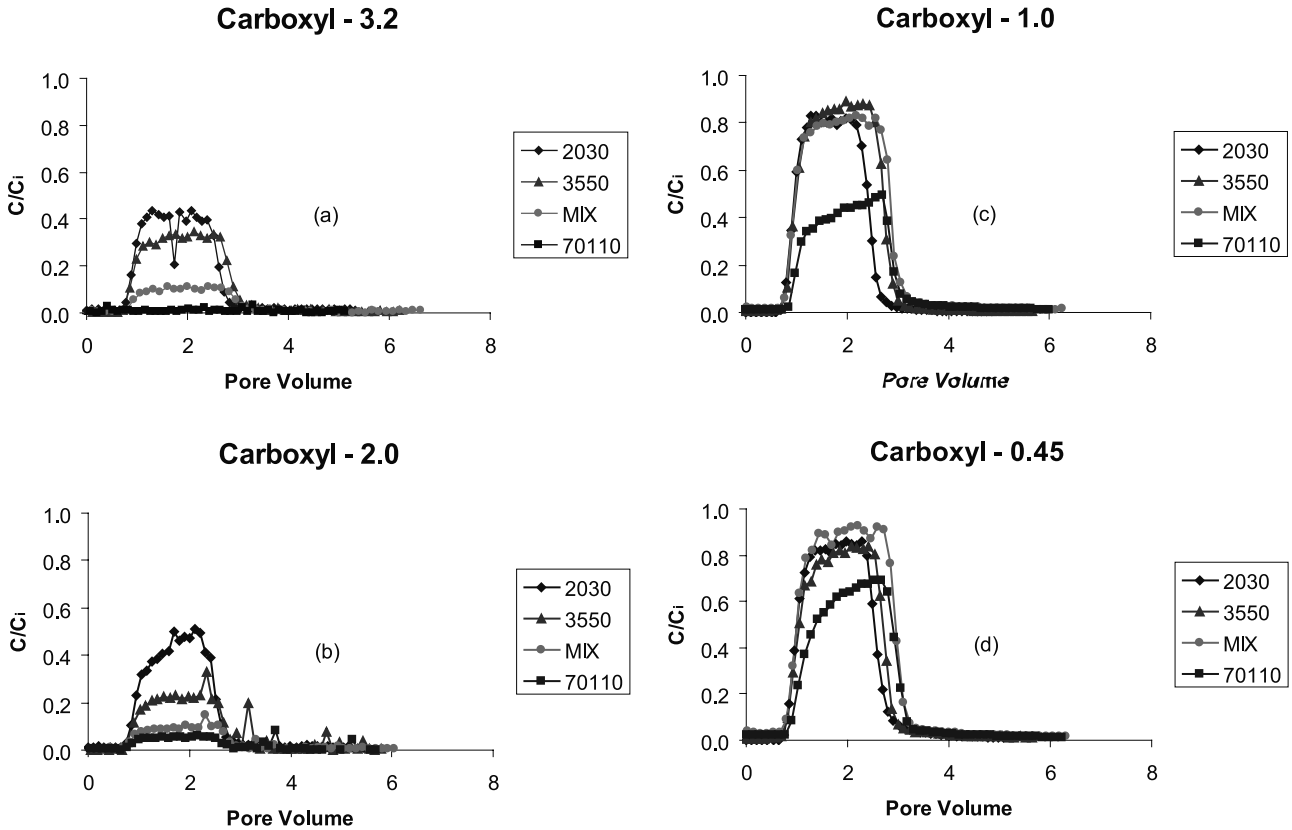

Figure 4. A plot of the relative colloid concentration in the effluent as a function of pore volume for the indicated colloid sizes (Figure 4a, 3.2 μm; Figure 4b, 2 μm; Figure 4c, 1 μm; and Figure 4d, 0.45 μm) and for the various soil types (2030, 3550, MIX, and 70110).

through time for the various colloid sizes is very similar to that of bromide. Furthermore, the peak colloid concentration decreases with increasing colloid size. Recall that the glass beads are chemically homogeneous, spherical, and smooth. Hence attachment of the carboxyl colloids (negatively charged) to the glass beads (negatively charged) cannot explain the observed effluent concentration curves. The high release efficiency of the colloids from the glass beads (see Table 3) also supports this hypothesis. All of these observations suggest that straining (increases with increasing colloid size) is the primary mechanism for colloid removal in these glass beads. Colloid transport experiments were also conducted for the various Ottawa sands described in Table 2. Figures 4a, 4b, 4c, and 4d present plots of the relative colloid concentration in the effluent as a function of pore volume for the 3.2, 2.0, 1.0, and 0.45 μm colloids, respectively, in the indicated sands. Bromide (Figure 2) and colloid (Figure 4) breakthrough times in a particular sand were quite similar. Differences in transport behavior of bromide and colloid particles increased with decreasing soil grain size and increasing colloid size. With decreasing soil grain size the peak effluent concentration was lower and the removal of a particular sized colloid enhanced. This is especially true for the larger 3.2 (Figure 4a) and 2.0 (Figure 4b) μm colloids; i.e., very little breakthrough occurs for the 3.2 μm colloids in the 70110 sand. Comparison of the effluent concentration curves for the different sized colloids in a particular sand also reveals a trend of lower peak effluent concentrations with increasing colloid size. Recall that similar behavior was observed for these same colloids in the glass beads (see Figure 3). All these results provide substantial evidence that straining can be an important removal mechanism for carboxyl colloids in these Ottawa sands.

[28] Comparison of Figures 4c and 4d reveals similar transport behavior for 1.0 and 0.45 μm colloids in 2030, 3550, and MIX sands. The peak effluent colloid concentration in these cases was around 80% of the initial influent concentration, and independent of the colloid and porous medium size. These observations suggest that little straining may be occurring over this range of colloid sizes and soil grain size distribution characteristics. In this case, mass removal is believed to be controlled by colloid attachment. Mechanisms of colloid attachment can be due to both chemical and physical (attachment at solid grain junction points and rough solid surfaces) processes. The exact mechanisms for colloid attachment cannot be deduced from the experimental data.

[29] The peak effluent concentration of the 1.0 (Figure 4c) and 0.45 (Figure 4d) μm colloids is lower in the finer 70110 sand than in the other Ottawa sands (2030, MIX, and 70110). Furthermore, a higher peak effluent concentration occurs for the 0.45 μm colloids ($C/C_i = 0.63$) than that for 1.0 μm colloids ($C/C_i = 0.48$) in the 70110 sand. These observations can again be attributed to enhanced straining with decreasing soil grain size and increasing colloid size. The effluent concentration curves for the 1.0 and 0.45 μm

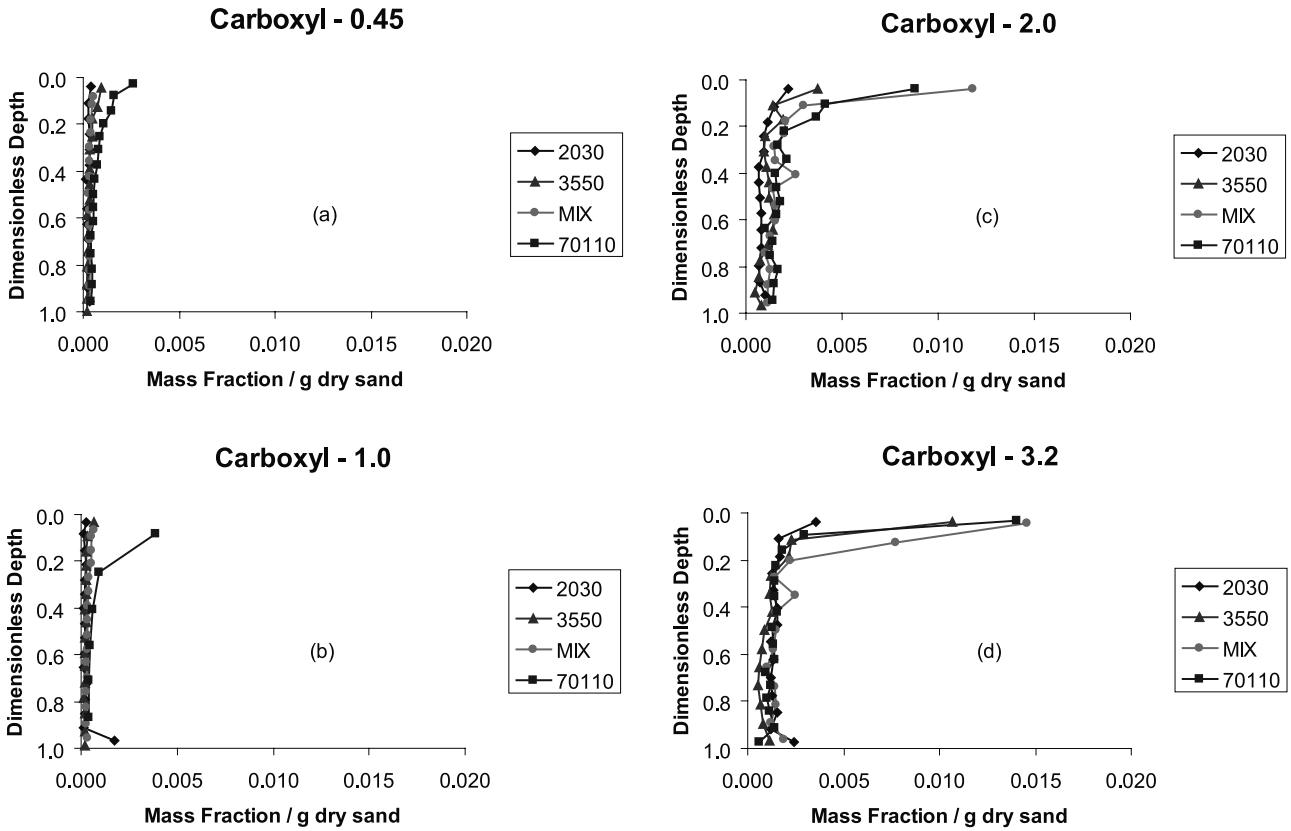

Figure 5. A plot of the fraction of total colloid mass per gram of dry sand as a function of normalized distance from the column inlet for the indicated colloid sizes (Figure 5a, 0.45 μm; Figure 5b, 1 μm; Figure 5c, 2 μm; and Figure 5d, 3.2 μm) and for the various soil types (2030, 3550, MIX, and 70110).

colloids in 70110 sand, and for the 2.0 μm colloids in 2030 sand (see Figure 4b), exhibit a much more gradual approach to their peak concentration value than the other curves shown in Figures 4a–4d. This behavior may be indicative of a superposition of straining and attachment processes and a transition from colloid straining to attachment.

[30] Table 2 indicates that the coefficient of uniformity for the glass beads and the MIX sand is quite different, whereas the mean grain size is very similar. Comparison of the effluent concentration curves for a particular sized colloid in the glass beads (Figure 3) and MIX sand (Figure 4) reveals that the peak effluent concentration was generally less in the glass beads than in the MIX sand. This result is attributed to differences in the soil grain size distribution characteristics. More colloid mass removal occurs in the uniform glass beads than in the graded MIX sands. Results from *Schaap and Bouten* [1996] indicate that grain and pore size (capillary pressure curves) distribution characteristics are positively correlated. The enhanced transport potential of colloids in the MIX sand is therefore believed to occur due to the presence of larger pores in the more graded MIX sand.

4.3. Spatial Distribution of Colloids

[31] After completion of the colloid tracer experiments, the remaining colloid mass in the sand was measured with distance from the soil column inlet. Figure 5 summarizes this data by presenting plots of the fraction of total colloid mass per gram of dry soil as a function of normalized distance from the column inlet for the various Ottawa sands. Specifically, Figures 5a, 5b, 5c, and 5d are for 0.45, 1.0, 2.0, and 3.2 μm colloids, respectively.

[32] Observe in Figure 5a that the fraction of 0.45 μm colloid mass retained in the soil tends to be more or less constant with distance for the 2030, 3550, and MIX soils. Recall from the discussion of Figure 4d that colloid removal in this case was attributed primarily to attachment. In contrast, observe in Figures 4d and 5a the behavior of the 0.45 μm colloids in 70110 sand. In this case, straining results in significant mass removal over the first few centimeters of soil from the inlet because blocked pores act as dead ends for the colloids. After the first few centimeters, colloids are only mobile in the larger continuous pore networks. Pore exclusion is hypothesized to inhibit further mass removal by straining in these networks, and colloid mass removal with depth therefore approaches a more uniform value. Since the magnitude of the retained colloids is similar to that of the other sands, it is hypothesized that attachment is the primary means of mass removal for dimensionless depths greater than 0.2. Comparison of Figures 5a and 5b indicates that very similar trends occur for the 1.0 and 0.45 μm colloids. This observation can again be explained by similarities in the removal mechanism for the colloids (see discussion for Figures 4c and 4d). Note, however, that for the 70110 soil a much higher mass fraction of 1.0 μm colloids (Figure 5b)

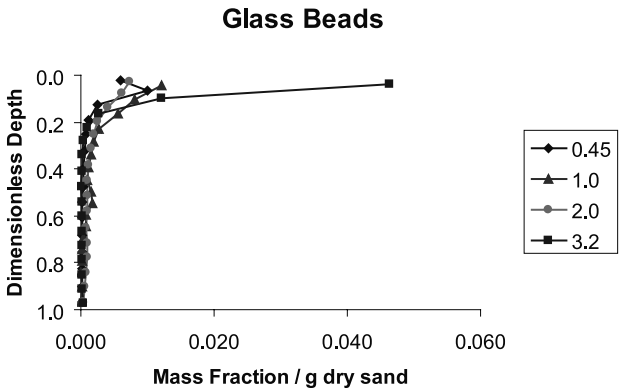

Figure 6. A plot of the fraction of total colloid mass per gram of dry porous media as a function of normalized distance from the column inlet for the variously sized colloids retained in the glass beads.

are removed in the first few centimeters of soil compared with the 0.45 μm colloids (Figure 5a). This is attributable to an increase in pore straining as a result of the increase in colloid size.

[33] For the larger colloid sizes, 2.0 (Figure 5c) and 3.2 (Figure 5d) μm, the primary mechanism for colloid removal by the soil is believed to be straining. Recall that straining increases with decreasing mean grain size. Hence the coarsest 2030 soil always exhibits the lowest colloid mass fractions at the column inlet, and the finest MIX and 70110 sands exhibit the highest colloid mass fractions at the column inlet. The 3550 sand shows intermediate behavior between these two extremes. After the initial sharp decrease in mass removal with increasing distance from the column inlet, note that the colloid mass fraction retained in the soil approaches a more constant value with depth (dimensionless depths greater than 0.2). In this region of more constant retention, pore exclusion may inhibit further mass removal by straining, and attachment is therefore believed to be the primary means of mass removal. To further support this hypothesis, note that the mass fraction of 3.2 and 2 μm colloids retained in the uniform concentration region is similar in magnitude to that for the 0.45 μm colloids.

[34] Comparison of the spatial distribution of various sized colloids in a particular sand reveals a trend of increasing colloid mass removal at the column inlet with increasing colloid size (see Figures 5a, 5b, 5c, and 5d). This result is again attributed to enhanced straining with increasing colloid size and is consistent with the observed effluent concentration curves shown in Figure 4.

[35] Figure 6 presents a plot of the spatial distribution of the variously sized colloids retained in the glass beads. The corresponding colloid effluent concentration curves were presented earlier in Figure 3. Notice that the mass fraction of retained colloids at the column inlet is greatest for the largest 3.2 μm colloids and is lowest for the smallest 0.45 μm colloids. This result is again attributed to enhanced straining with increasing colloid size. The 1.0 and 2.0 μm colloids exhibit intermediate behavior to these two extremes. Similar colloid mass distributions occur for the 1.0 and 2.0 μm colloids occur because of their comparable effluent concentration curves (see Figure 3). In all cases, the concentration of retained colloids is relatively low and constant for dimensionless depths greater than 0.2. As for the Ottawa sand, this result is ascribed to pore exclusion that limits straining.

[36] Recall that the mean grain size of the MIX sand and the glass beads is quite similar, whereas the coefficient of uniformity is very different (see Table 2). Comparison of the spatial distribution of a particular sized colloid in the MIX sand (Figure 5) and glass beads (Figure 6) reveals more colloid retention at the column inlet in the glass beads than in the MIX sand. This is indicative of enhanced straining in the glass beads. The uniform glass beads are believed to have fewer large pores than the graded MIX sands. Differences in the effluent concentration curves also support this hypothesis (see Figures 3 and 4).

4.4. Simulating Colloid Transport

[37] Colloid attachment theory has been used to predict colloid transport behavior for a wide variety of colloid and porous media characteristics. Recall that equations (1)–(3) were developed under the assumption that attachment controls colloid mass removal by porous media. Little attention has been paid to the colloid and porous media parameter ranges that may limit attachment model applicability, because colloid straining has been assumed a priori to be insignificant. Colloid attachment theory is not designed to quantify colloid mass removal via straining. Comparison of the attachment model results and experimental data will be used herein to highlight differences in colloid attachment and straining behavior and to help identify parameter ranges that are applicable for attachment models.

[38] A slightly modified version of the Hydrus-1D computer code [*Simunek et al.*, 1998] was utilized to simulate the colloid transport experiments. Hydrus-1D simulates water, heat, and multiple solute movement in one-dimensional variably-saturated porous media. The code is coupled to a nonlinear least squares optimization routine based upon the Marquardt-Levenberg algorithm [*Marquardt*, 1963] to facilitate the estimation of solute transport parameters from

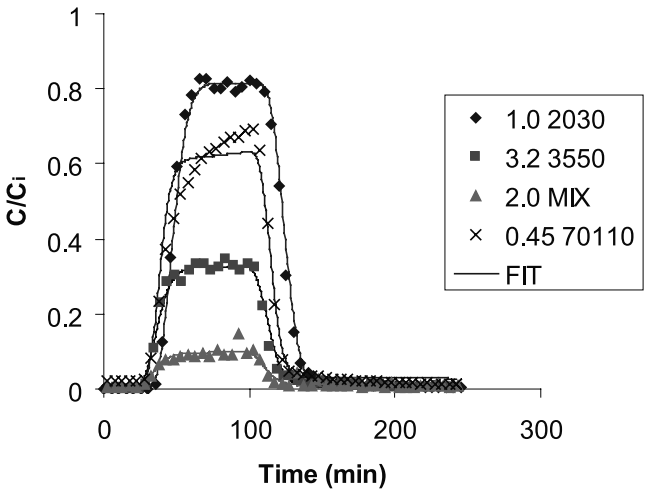

Figure 7. Observed and fitted (λ_H, k_{att}, and k_{det}) effluent concentration curves for several representative colloid transport experiments indicated in the legend.

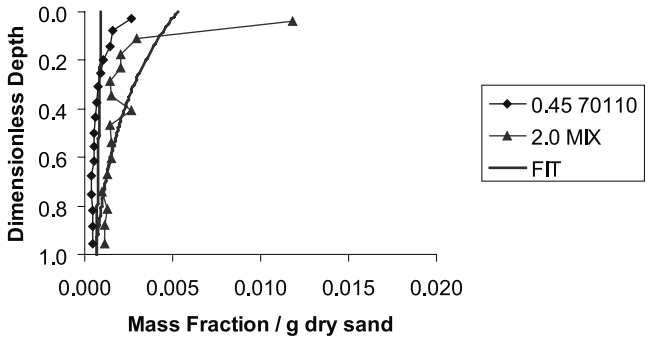

Figure 8. Observed and simulated fraction of total colloid mass per gram of dry soil as a function of normalized distance from the column inlet for several representative systems indicated in the legend.

experimental data. Attachment and detachment rate coefficients, and the hydrodynamic dispersivity (λ_H) were simultaneously fitted to each colloid effluent concentration curve. Since bromide and colloids may not necessarily follow the same flow paths, a separate bromide tracer hydrodynamic dispersivity (λ_H^{BR}) was also fitted to the experimental data.

[39] Figure 7 presents the observed and fitted effluent concentration curves for several representative colloid transport experiments. Observe that the simulation fits describes the experimental data fairly well. The fit of the data for 0.45 μm colloids in 70110 sand is described less adequately than the other data shown in Figure 7. Here the experimental data exhibit a more gradual approach to its peak effluent concentration value. Detachment cannot account for this behavior because a higher detachment rate would also lead to higher concentration tailing. The asymmetric shape of the effluent concentration curve for 0.45 μm colloids in 70110 sand is therefore believed to reflect a transition from colloid attachment to straining.

[40] Figure 8 presents the observed and simulated fraction of total colloid mass per gram of dry soil as a function of normalized distance from the column inlet for several representative systems. Observe that the simulated decrease in the colloid concentration with depth is much more gradual than that shown by the experimental data. This is especially true for systems in which significant colloid mass was retained by the soil as a result of straining. For example, observe the difference between simulated and experimental 2 μm colloids in MIX sand compared to 0.45 μm colloids in 70110 sand. Although the effluent concentration curves shown in Figure 7 were adequately described using a first-order attachment and detachment coefficient, Figure 8 suggests that this modeling approach does not describe the observed spatial colloid distribution well for systems that exhibit significant straining.

[41] Table 4 presents the estimated parameters values of λ_H^{BR}, λ_H, k_{att}, and k_{det} as well as the correlation coefficient. Observe that values of λ_H^{BR} and λ_H are significantly different for a particular experimental system, with λ_H^{BR} tending to be less than λ_H. The higher λ_H value may occur to compensate for the inability of the colloid attachment theory to perfectly describe the data. Alternatively, the higher λ_H values may also indicate that the colloid particles experience more spreading in the soil and follow a slightly different flow path than bromide due to pore exclusion of colloids. Consistent with colloid straining, the value of k_{att} tends to increase with increasing colloid size (for a particular porous medium) and decreasing mean grain size (for a particular colloid size). Table 4 also indicates that higher values of k_{det} occur for the smaller sized colloids. Recall that attachment was hypothesized to be the dominant mechanism of mass removal for the smaller sized colloids.

[42] Table 4 also presents calculated values of η according to equation (3). The value of η, for a particular soil type, is predicted to be maximum for the smallest (0.45 μm) colloids and tends to achieve a minimum value for the 2.0 μm colloids. The attachment coefficients given in Table 4, however, tend to reach a maximum value for the largest colloids. To compensate for this difference, values of α (as determined from equation (2) using the values of η and k_{att} given in Table 4) vary with colloid size and soil type. Recall that α theoretically accounts for the net effect of repulsive

Table 4. Fitted (Bromide Dispersivity, λ_H^{BR}; Colloid Dispersivity, λ_H; Attachment Coefficient, k_{att}; Detachment Coefficient, k_{det}; and Colloid Sticking Efficiency, α) and Calculated (Collector Efficiency, η) Model Parameters

Soil Type	d_p, μm	λ_H^{BR}, cm	λ_H, cm	$k_{att} \times 10^3$, min^1	$k_{det} \times 10^4$, min^1	$\eta \times 10^2$	$\alpha \times 10^2$	r^2
2030	0.45	0.080	0.189	3.75	30.2	2.87	3.59	0.998
2030	1.00	0.061	0.237	4.01	0.75	1.80	6.33	0.986
2030	2.00	0.092	0.110	20.1	10.6	1.81	29.8	0.974
2030	3.20	0.076	0.239	19.3	4.10	2.87	17.6	0.990
3550	0.45	0.070	0.151	5.46	21.5	4.80	1.43	0.997
3550	1.00	0.070	0.158	3.57	6.65	3.00	1.48	0.998
3550	2.00	0.148	0.493	36.9	8.61	2.60	17.4	0.885
3550	3.20	0.103	0.288	29.7	2.87	3.48	10.4	0.991
MIX	0.45	0.094	0.095	3.06	45.4	6.28	0.37	0.997
MIX	1.00	0.074	0.179	56.8	10.0	3.91	10.9	0.992
MIX	2.00	0.105	0.385	63.0	6.00	3.14	15.7	0.929
MIX	3.20	0.053	0.361	63.0	3.75	4.04	11.7	0.984
70110	0.45	0.104	0.166	12.8	14.4	8.02	0.75	0.985
70110	1.00	0.080	0.071	22.2	12.4	5.22	2.09	0.981
70110	2.00	0.071	0.299	77.0	7.09	4.29	8.91	0.726
70110	3.20	0.179	0.355	132.2	24.0	5.14	12.9	0.001
GB	0.45	0.260	0.135	14.9	0.02	4.44	2.51	0.988
GB	1.00	0.086	0.091	81.9	20.1	2.70	19.1	0.941
GB	2.00	0.209	0.122	102.1	13.5	2.00	30.7	0.927
GB	3.20	0.047	0.100	232.9	7.18	2.68	59.9	0.094

and attractive forces between colloids and solid surfaces. Since the electrostatic forces between the various sized carboxyl colloids (see Table 1) and Ottawa sands are similar in magnitude, the scatter in calculated values of α (2 orders of magnitude) reflects the inability of this approach to predict the experimental data. *Ryan and Elimelech* [1996] also noted serious discrepancies between calculated sticking efficiencies and experimentally measured values. This limitation may occur in part because straining is not adequately described by this theory.

[43] The numerical simulations demonstrate that traditional colloid attachment theory is not well suited to describe colloid transport in systems that exhibit straining. The experimental data strongly suggest that straining is an important mechanism of colloid retention for the larger 2.0 and 3.2 μm colloids in the various porous media considered herein. Colloid straining also likely occurred for the 0.45 and 1.0 μm colloids in the finest 70110 sand and the glass beads. Caution is therefore warranted when applying colloid attachment theory to colloids and porous media that encompass this range in size; i.e., when the ratio of the colloid diameter to the mean grain diameter (d_p/d_{50}) is greater than approximately 0.0017.

[44] The colloid transport studies presented herein were conducted in water-saturated porous media and with negatively charged colloids. In unsaturated systems, water flow and colloid transport will be controlled by the spatial distribution of water saturation. At lower water saturations, water flow occurs primarily in the finer grained materials, and smaller pores and pore spaces. Hence the significance of the physical factors (colloid size and grain size distribution) is anticipated to be magnified in unsaturated systems. Straining may also be influenced by other physical (water velocity, colloid concentration, colloid and soil grain size distribution characteristics, heterogeneity, and dimensionality) and chemical (surface charge of colloid and porous media) factors of the porous media and colloids. Additional colloid transport studies are currently under way to quantify these transport processes and to incorporate these findings into a deterministic colloid transport simulator.

References

Ayers, R. S., and D. W. Westcot, Water quality for agriculture, *FAO Irrig. and Drain. Pap.,29*, *Rev.*1, U.N. Food and Agric. Organ., Rome, 1989.

Bales, R. C., S. R. Hinkle, T. W. Kroeger, and K. Stocking, Bacteriophage adsorption during transport through porous media: Chemical perturbations and reversibility, *Environ. Sci. Technol.*, *25*, 2088–2095, 1991.

Bettahar, M., O. Razakarisoa, F. van Dorpe, and M. Baviere, Influence of a surfactant decontamination technique on the hydraulic conductivity of a controlled aquifer polluted by diesel oil, *Rev. Sci. Eau*, *11*, 85–100, 1998.

Bitton, G., and R. W. Harvey, Transport of pathogens through soil, in *New Concepts in Environmental Microbiology*, edited by R. Mitchell, pp. 103–124, John Wiley, New York, 1992.

Bolster, C. H., A. L. Mills, G. M. Hornberger, and J. S. Herman, Spatial distribution of bacteria experiments in intact cores, *Water Resour. Res.*, *35*, 1797–1807, 1999.

Bradford, S. A., and L. M. Abriola, Dissolution of residual tetrachloroethylene in fractional wettability porous media: Incorporation of interfacial area estimates, *Water Resour. Res.*, *37*, 1183–1195, 2001.

Corapcioglu, M. Y., and H. Choi, Modeling colloid transport in unsaturated porous media and validation with laboratory column data, *Water Resour. Res.*, *32*, 3437–3449, 1996.

Danielson, R. E., and P. L. Sutherland, Porosity, in *Methods Soil Analysis,-Part 1: Physical and Mineralogical Methods*, 2nd ed., edited by A. Klute, pp. 443–461, Soil Sci. Soc. of Am., Madison, Wisc., 1986.

Elimelech, M., and C. R. O'Melia, Kinetics of deposition of colloidal particles in porous media, *Environ. Sci. Technol.*, *24*, 1528–1536, 1990.

Fitzpatrick, J. A., and L. A. Spielman, Filtration of aqueous latex suspensions through beds of glass spheres, *J. Colloid Interface Sci.*, *43*, 350–369, 1973.

Gschwend, P. M., and M. D. J. Reynolds, Monodisperse ferrous phosphate colloids in an anoxic groundwater plume, *J. Contam. Hydrol.*, *1*, 309–327, 1987.

Harvey, R. W., and S. P. Garabedian, Use of colloid filtration theory in modeling movement of bacteria through a contaminated sandy aquifer, *Environ. Sci. Technol.*, *25*, 178–185, 1991.

Harvey, R. W., N. E. Kinner, D. MacDonald, D. W. Metge, and A. Bunn, Role of physical heterogeneity in the interpretation of small-scale laboratory and field observations of bacteria, microbial-sized microsphere, and bromide transport through aquifer sediments, *Water Resour. Res.*, *29*, 2713–2721, 1993.

Herzig, J. P., D. M. Leclerc, and P. LeGoff, Flow of suspension through porous media: Application to deep filtration, *Ind. Eng. Chem. Res.*, *62*, 129–157, 1970.

Johnson, P. R., and M. Elimelech, Dynamics of colloid deposition in porous media: Blocking based on random sequential adsorption, *Langmuir*, *11*, 801–812, 1995.

Kim, J. I., Actinide colloid generation in groundwater, *Radiochim. Acta*, *52/53*, 71–81, 1991.

Kretzschmar, R., K. Barmettler, D. Grolimund, Y.-D. Yan, M. Borkovec, and H. Sticher, Experimental determination of colloid deposition rates and collision efficiencies in natural porous media, *Water Resour. Res.*, *33*, 1129–1137, 1997.

Logan, B. E., D. G. Jewett, R. G. Arnold, E. J. Bouwer, and C. R. O'Melia, Clarification of clean-bed filtration models, *J. Environ. Eng.*, *121*, 869–873, 1995.

MacCarthy, J. F., and J. M. Zachara, Subsurface transport of contaminants, *Environ. Sci. Technol.*, *23*, 496–502, 1989.

MacLeod, F. A., H. M. Lappin-Scott, and J. W. Costerton, Plugging of a model rock system by using starved bacteria, *Appl. Environ. Microbiol.*, *54*, 1365–1372, 1988.

Marquardt, D. W., An algorithm for least-squares estimation of nonlinear parameters, *J. Soc. Ind. Appl. Math.*, *11*, 431–441, 1963.

Matthess, G., and A. Pekdeger, Survival and transport of pathogenic bacteria and viruses in groundwater, in *Ground Water Quality*, edited by C. H. Ward, W. Giger, and P. McCarty, pp. 472–482, John Wiley, New York, 1985.

McDowell-Boyer, L. M., J. R. Hunt, and N. Sitar, Particle transport through porous media, *Water Resour. Res.*, *22*, 1901–1921, 1986.

Nyhan, J. W., B. J. Brennon, W. V. Abeele, M. L. Wheeler, W. D. Purtymun, G. Trujillo, W. J. Herrera, and J. W. Booth, Distribution of plutonium and americium beneath a 33-yr-old liquid waste disposal site, *J. Environ. Qual.*, *14*, 501–509, 1985.

Ouyang, Y., D. Shinde, R. S. Mansell, and W. Harris, Colloid-enhanced transport of chemicals in subsurface environments: A review, *Crit. Rev. Environ. Sci. Technol.*, *26*, 189–204, 1996.

Pieper, A. P., J. N. Ryan, R. W. Harvey, G. L. Amy, T. H. Illangasekare, and D. W. Metge, Transport and recovery of bacteriophage PRD1 in a sand and gravel aquifer: Effect of sewage-derived organic matter, *Environ. Sci. Technol.*, *31*, 1163–1170, 1997.

Puls, R. W., and R. M. Powell, Transport of inorganic colloids through natural aquifer material: Implications for contaminant transport, *Environ. Sci. Technol.*, *26*, 614–621, 1992.

Rajagopalan, R., and C. Tien, Trajectory analysis of deep-bed filtration with the sphere-in-a-cell porous media model, *AIChE J.*, *22*, 523–533, 1976.

Redman, J. A., S. B. Grant, T. M. Olson, M. E. Hardy, and M. K. Estes, Filtration of recombinant Norwalk virus particles and bacteriophage MS2 in quartz sand: Importance of electrostatic interactions, *Environ. Sci. Technol.*, *31*, 3378–3383, 1997.

Redman, J. A., S. B. Grant, T. M. Olson, and M. K. Estes, Pathogen filtration, heterogeneity, and the potable reuse of wastewater, *Environ. Sci. Technol.*, *35*, 1798–1805, 2001.

Reimus, P. W., The use of synthetic colloids in tracer transport experiments in saturated rock fractures, *Rep. LA-13004-T*, Los Alamos Natl. Lab., Los Alamos, N. M., 1995.

Ryan, J. N., and M. Elimelech, Colloid mobilization and transport in groundwater, *Colloids Surf. A*, *107*, 1–56, 1996.

Ryan, J. N., and P. M. Gschwend, Colloid mobilization in two Atlantic coastal plan aquifers: Field studies, *Water Resour. Res.*, *26*, 307–322, 1990.

Ryan, J. N., M. Elimelech, R. A. Ard, R. W. Harvey, and P. R. Johnson, Bacteriophage PRD1 and silica colloid transport and recovery in an iron oxide-coated sand aquifer, *Environ. Sci. Technol.*, *33*, 63–73, 1999.

Sakthivadivel, R., Theory and mechanism of filtration of non-colloidal fines through a porous medium, *Rep. HEL 15-5*, 110 pp., Hydraul. Eng. Lab., Univ. of Calif., Berkeley, 1966.

Sakthivadivel, R., Clogging of a granular porous medium by sediment, *Rep. HEL 15-7*, 106 pp., Hydraul. Eng. Lab., Univ. of Calif., Berkeley, 1969.

Schaap, M. G., and W. Bouten, Modeling water retention curves of sandy soils using neural networks, *Water Resour. Res.*, *32*, 3033–3040, 1996.

Schijven, J. F., and S. M. Hassanizadeh, Removal of viruses by soil passage: Overview of modeling, processes, and parameters, *Crit. Rev. Environ. Sci. Technol.*, *30*, 49–127, 2000.

Simunek, J., K. Huang, M. Sejna, and M. T. van Genuchten, The HYDRUS-1D software package for simulating the one-dimensional movement of water, heat, and multiple solutes in variably-saturated media -version 1.0, *IGWMC-TPS-70*, 186 pp., Int. Ground Water Model, Cent., Colo. School of Mines, Golden, Colo., 1998.

Tobiason, J. E., and C. R. O'Melia, Physicochemical aspects of particle removal in depth filtration, *J. Am. Water Works Assoc.*, *80*, 54–64, 1988.

Vaidyanathan, R., and C. Tien, Hydrosol deposition in granular media under unfavorable surface conditions, *Chem. Eng. Sci.*, *46*, 967–983, 1991.

Van Genuchten, M. T., Determining transport parameters from solute displacement experiments, *Res. Rep. 118*, U.S. Dep. of Agric., Sci. and Educ. Admin., U.S. Salinity Lab., Riverside, Calif., 1980.

Wan, J., and J. L. Wilson, Visualization of the role of the gas-water interface on the fate and transport of colloids in porous media, *Water Resour. Res.*, *30*, 11–23, 1994a.

Wan, J., and J. L. Wilson, Colloid transport in unsaturated porous media, *Water Resour. Res.*, *30*, 857–864, 1994b.

Willis, M. S., and I. Tosun, A rigorous cake filtration theory, *Chem. Eng. Sci.*, *35*, 2427–2438, 1980.

Wilson, J. T., L. E. Leach, M. Henson, and J. N. Jones, In situ biorestoration as a ground water remediation technique, *Ground Water Monit. Rev.*, *6*, 56–64, 1986.

M. Bettahar, S. A. Bradford, J. Simunek, and S. R. Yates, George E. Brown, Jr., Salinity Laboratory, U.S. Department of Agriculture, Agricultural Research Service, 450 W. Big Springs Road, Riverside, CA 92507-4617, USA. (sbradford@ussl.ars.usda.gov)